

Surface cracks growth for superalloy in a round bar under different loading

M. Abdulrazzaq¹, Mahmoud. A. Hassan²

¹Department of Materials Engineering, College of Engineering, University of Al-qadisiyah, Iraq, Mohammed.Abbood@qu.edu.iq

²Department of Mechanical Engineering, College of Engineering, University of Al-qadisiyah, Iraq, Mahmoud.Hassan@qu.edu.iq

Received: 21-02-2023

Accepted: 31-03-2023

Abstract: The main objective of this paper is to experimentally and numerically detect the surface cracks in the round bar for Ni-Al- 315 steel superalloy and calculate the crack depth which induces the sintering of these alloys. Several factors have contributed to surface defects, such as metallurgical defects and notches. The surface crack orientation can be estimated at the observed crack increase by using displacement. Various crack aspect ratios, a/b , ranging from 0.0 to 1.0, and relative crack depth, a/D , ranging from 0.2 to 0.4, are considered. The superalloy (Ni, Al and 315 steel) has been successfully modified utilizing the powder metallurgical process. The specimens are typically made up of Six layers, starting with (Al, Ni) across one side and ending with (Ni-Al- 315 steel) on another. Transmission electron microscopy (SEM) Instrument analysis has been used to detect the surface cracks and analyze the microstructure of superalloy used in detail using the X-pert analytical program.

Keywords: crack depth; alloys.

1. Introduction

Cylindrical applications such as a round bar successfully transmit mechanical energy. Failure of this equipment is subjected to wrong loads and may induce mechanical damage, which happens not only to single loads but also to combined loads. The round bar in service is subject to mixed load due to self-weight, which induces the shaft to bend, causing failure and the appearance of surface cracks in the bar. Also, the applications are practically exposed to different loading kinds like torsion, tension and shear subsequent in a mixed-load interface. Therefore, the stress state of the crack tip is usually created by arranged combined loading type of interactions. Hence, the cracks can grow in a round bar's surface and may be subject to failure. Usually, crack initiation should be related to factors (SIFs) in the complex state [1; 2]. Crack imitation analysis is necessary for several fields since fatigue cracks are a significant source of failures [3]. Therefore, in many applications, the notch path is accurate and estimated fatigue life is of fundamental importance in terms of reliability [4]. Many factors contributed to the appearance to initiate surface cracks [5]. Under linear elastic analysis, the concepts of (SI factors) are effectively utilized as driving fracture coefficients. Although, once a substantial amount of plastic deformation has occurred, the application of this parametric ether collapse [6]. Ductile metal components can withstand stress caused by rapid temperature fluctuations in

a short time [7; 8]. The volume or weight percentage, configuration, and geometry of changes in phase distribution can all be converted. The difference in volume fraction might occur in any direction or immediately over the component's total thickness, such as the bar. Because of its modest expansion capacity, the ceramic area has high heat resistance. Ductile metal components can withstand stress caused by rapid temperature fluctuations in a short time [9; 10].

Composite materials provide a higher strength-to-stiffness ratio, better fatigue, wear, and corrosion resistance, and higher dependability than pure or alloyed metals. Despite these benefits, composite materials have an abrupt shift of characteristics at the interface, which can lead to components failure by (delamination) under extreme operating conditions. Delamination is a failure mode in which a material cracks into layers. Delamination may occur in several materials, such as multilayer composites [7] and concrete. Superalloy is a revolutionary hybrid material that tailors material properties to individual application requirements, revolutionizing materials research.

Nevertheless, there are still roadblocks in the way of achieving this objective. Other challenges include a lack of data obtained, technology such as mass production to leverage this approach properly., and so on, in addition to the primary cost issue. This composition gradient significantly strengthened the resistance to transverse crack propagation under impact stress [11]. It was utilized in developing electrodes using energy storage applications because of its versatility in controlling its thickness and the shape of the deposited layer [12]. The procedures listed down are the first phases in the PM method for making green compressed. The prior sintered green compressed powder is prepared, blended for appropriate ingredients, and layered or compressed for consolidating by mechanical pressing or hot compressing. Sintering is the process of heating powder below its melting temperature in a furnace, causing atom diffusion and resulting in atom bonding to create a heavy compact with tight adhesion among metal powder [13; 14]. Table 1 depicts the overall evolution of the powder metallurgy approach through detailed many authors' superalloys fabrication work, as well as the material combinations used— macroscopic objects and heterogeneous Compounds with no flaw at the interface, as shown in optical micrographs. The effect of stress distributions in the specimen described the mechanism behind crack development, deflection, and spallation.

After sintering, superalloy annealed components showed increased thermoelectric characteristics, a dense structure, and a high carrier concentration. The electronic format characteristics depend on the processing condition, and atomic defects and local strains are formed due to the alloy's circumstances. Annealing has been used to lessen or remove this problem by stabilizing its thermo-electric behaviour [15]. Flaws or faults in the material, such as microcracks or pores, can complicate the modelling of layered materials. It is essential to include these characteristics while modelling the structure or component. Multi-site cracks are always present before a component fracture. These cracks' fracture tip stress fields interact [16; 17].

2. Material preparation

Nickel and aluminum powders were used as raw materials to make the superalloy in this section. The matrix materials were as-atomized Al powders (99.8% purity), including a mean particle size of 18.3 μ . Steel 315 powder samples with a mean particle size of 45 microns were used as toughness reinforcements, and Nickel powder samples with a mean particle size of 9.922 μ were used as reinforcements. Table 1 illustrates the basic powder properties which are used.

Table. 1 *The property specification of the powders*

Property	Size(μm)	$\rho(\text{g/cm}^3)$	Purity (%)
Aluminium	18.3	2.79	99
Nickle	9.922	8.9	99.8
315 steels	45	7.8	compound

Six layers consist of the alloy sample. All the initial layers 2mm thick are created by (%33.3 Ni, %33.3Al, %33.3 315 Steel). Each layer's ingredients are combined according to a pre-determined compound weight (0.99 gm). The Milling could be done in solid shaker crushers, in which small quantities of about 10 to20 g have been milled at quite a period, primarily by alloy inspection, or in lesser planetary Milling, in which large amounts of particles (approximately 200 g) could be shredded, or in attritors, where even larger quantities can be milled at once. Shaker crushers operate within about 1200 rev/min, radial mills at 150 to 600 rev/min, and powder at 100 to 200 rpm. Then, utilizing the vacuum furnace and an argon environment, all green-produced compact alloy samples were sintered at 600 °C. The spaceman was sintered by warming, then to 400°C at a rate of 10°C/min for one hour, then to 620° C for three hours. The heating rate was less than ten °C/min throughout the process. Sintering is a process that increases the strength of a compressed bar. An argon gas environment furnace was used for the sintering process. The temperature change in the furnace-like time-dependent during the sintering temperature. All zinc stearate in the sample evaporates almost completely at 335°C, and the structure is destroyed after sintering. During sintering, argon gas is provided at a steady flow rate of 50 ml/min to prevent aluminium from oxidizing. The model geometry configuration round bar that is homogenous and axially stacked is studied using the experimental model and a hydraulic press. The prepared powder combination is cold compressed in a die at 780 MPa. Figure1. shows a round bar sample after cold pressing.

**Figure 1.** *A round bar sample after cold pressing.*

All zinc stearate in the sample evaporates almost completely at 335°C, and the structure is destroyed after sintering. During sintering, argon gas is provided at a steady flow rate of 50 ml/min to prevent aluminum from oxidizing. Figure. 2 depicts the final shape of the beam samples.

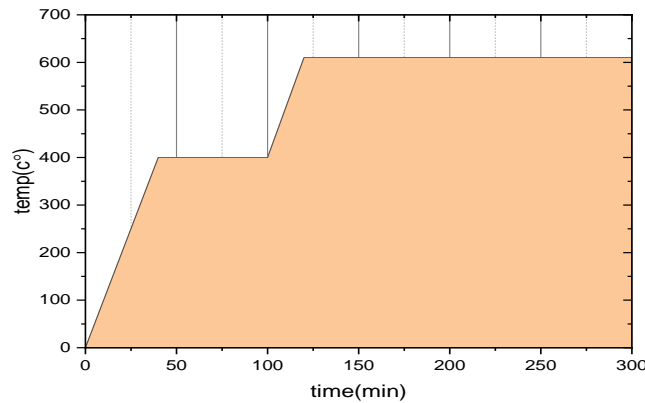


Figure 2. The sintering process temperature /time.

3. Results and Discussion

The mechanical behaviour of Aluminum-Nickel-315 steel alloy was tested experimentally according to ASTM E-8M standard. The specimen was examined for load-crack formation movement and load-stretching, and the moment of torsion T_x and moment of bending M_y were recorded. Table .2 shows the stiffness and toughness values for the sample. Toughness is measured using Linear Fracture Mechanics (LEFM) concepts and the structural hardness characteristics, according to ASTM E.8 standards testing protocol.

Table. 2 Stiffness and toughness values for the sample.

No. sample	Stiffness(k) N/mm	Toughness J·m ⁻³
1	89.22	40350. 75

The independent node attached to the model using a round bar element. This node receives the direct application of the moment of torsion and moment of bending. While the axial load to the x direction over the cross-section of a round bar. Following the determination of the elastic FE solution to the specific problem, nodal deformations along two crack faces are identified and used to compute the SIFs as follows.

$$K_I = \sigma \sqrt{\pi a}$$

$$K_I = \sqrt{\sec \pi a W} \sigma \sqrt{\pi a}$$

$$K_I = 1.12 \sigma \sqrt{\pi a}$$

Where the SIF has been reduced along the crack front, deeper cracks at $a/b = 1.0$ can improve the integrity of the bar when subjected to torsion forces. Tables 3 and 4 contain a list of all the SIFs obtained from pure torsion and tension.

Table 3. Normalized SIFs obtained from bending moment

a/b

a/D	0.0	0.2	0.4	0.6	0.8	1.0
0.2	0.0015	0.0019	0.0012	0.0014	0.0024	0.0016
0.3	0.0019	0.0018	0.0016	0.0023	0.0018	0.0018
0.4	0.0023	0.0017	0.0019	0.0021	0.0020	0.0026

Table 4. Normalized SIFs obtained from torsion moment

a/D	a/b					
	0.0	0.2	0.4	0.6	0.8	1.0
0.2	0.7654	0.700	0.6222	0.5881	0.5230	0.4901
0.3	0.7023	0.6091	0.5786	0.5344	0.4754	0.4541
0.4	0.6782	0.5987	0.5231	0.5010	0.4230	0.4411

Crack behavior under different moments shows the bar under the torsion moment does not open as wide as the bending moment shown in Figure 3,4. In the FE method analysis, the (SIFs) are calculated concerning the relative distance obtained under bending and torsional load. Furthermore, the round bar condition becomes non-symmetric distribution around the tip of the crack notch, which is supported a build a complete FE method. This paper presents the results of an SEM investigation of the surface crack of a superalloy specimen made from nickel, aluminum, and steel alloy. The initiation and growth of cracks were monitored throughout different loading.

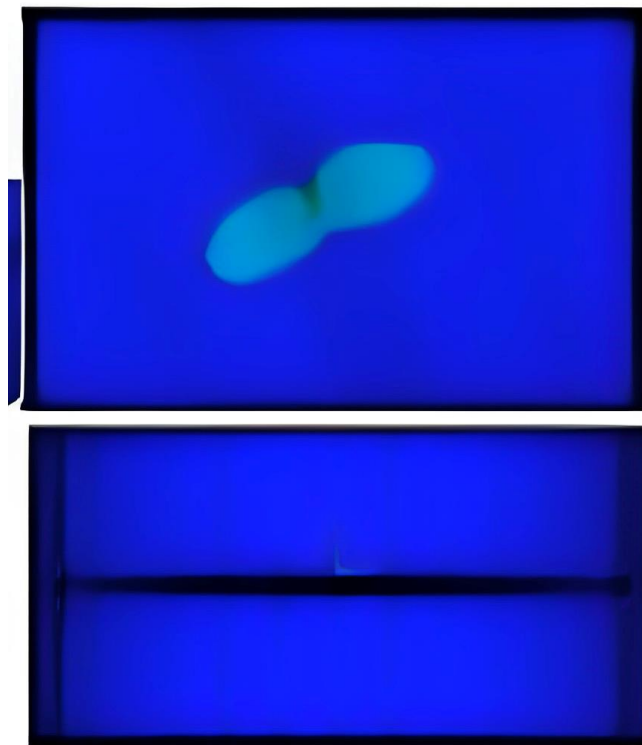


Figure 3. Under bending moment

On the surfaces of the specimens, the orientations of minor crack initiation and propagation were noticed. The JEOL 6480LV instrument was used to capture the SEM images, to which a special working table was mounted to allow for vertical specimen gripping and tilting. Even though it is employed after the experiment, the SEM surface crack analysis gives information on the events occurring inside the material. Figure 5 shows the surface crack of a specimen subjected to axial loading. The fragments are marked, and the discussion of them follows. Figure 5 (a) shows the piece where the start of a minor crack coalescing was noted at the surface.

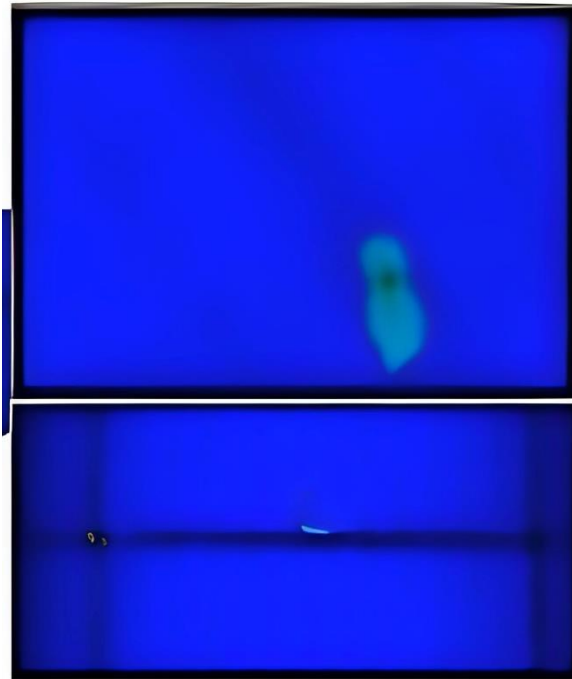


Figure 4. *Under torsion moment*

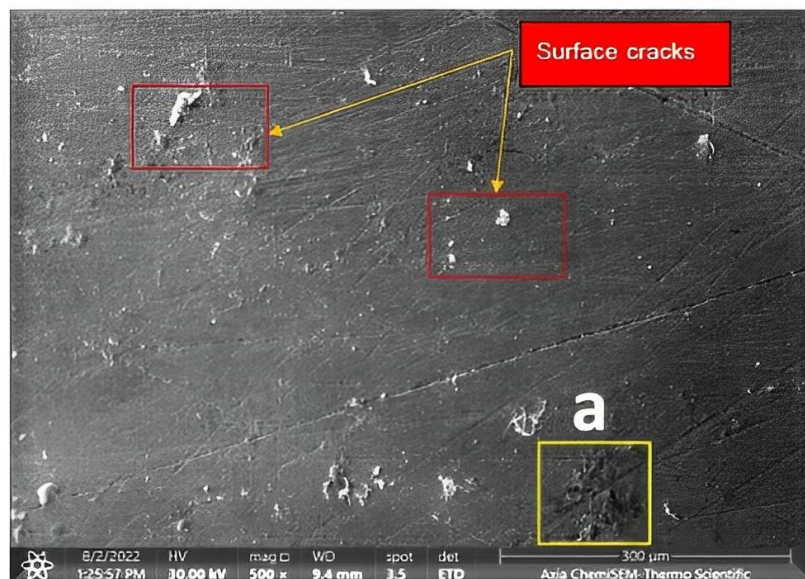


Figure 5. *SEM picture of the surface crack in the specimen*

4. Conclusion

FE method analyses were achieved for surface cracks in round bars under different loadings. According to the read-write reading, different solutions were found to calculate the SIFs measured under bending and torsion loadings are available. It was expected that the SIFs could calculate the different loading together. The cause of FE is due to the mechanisms shown by the deformed notches, where the surface cracks. Additionally, the surface crack opening under different loadings increases the relative node distances. 315 steel addition enhances the mechanical characteristics of the Al-Ni alloy. When the value of 315 steel and particle concentration is raised, the mechanical properties of the superalloy are improved. Compared to steel structural elements, they are more efficient, lighter than average, and less expensive.

References

- [1] Anderson, T. L. (2017). *Fracture mechanics: fundamentals and applications*. CRC press.
- [2] Testing, A. S. f., Fatigue, M. C. E. o., & Fracture. (2008). Standard test method for measurement of fatigue crack growth rates.
- [3] Gomes, G., & Miranda, A. C. (2018). Analysis of crack growth problems using the object-oriented program bemcracker2D. *Frattura ed Integrità Strutturale*, 12(45), 67-85.
- [4] Chen, H., Wang, Q., Zeng, W., Liu, G., Sun, J., He, L., & Bui, T. Q. (2019). Dynamic brittle crack propagation modeling using singular edge-based smoothed finite element method with local mesh rezoning. *European Journal of Mechanics-A/Solids*, 76, 208-223.
- [5] Yan, X., & Liu, B. (2011). A numerical analysis of cracks emanating from a surface elliptical hole in infinite body in tension. *Meccanica*, 46, 263-278.
- [6] Benedetti, M., Beghini, M., Bertini, L., & Fontanari, V. (2008). Experimental investigation on the propagation of fatigue cracks emanating from sharp notches. *Meccanica*, 43, 201-210.
- [7] Bhavar, V., Kattire, P., Thakare, S., & Singh, R. (2017). A review on functionally gradient materials (FGMs) and their applications. IOP conference series: materials science and engineering,
- [8] CPM, S. A., Varghese, B., & Baby, A. (2014). A review on functionally graded materials. *Int. J. Eng. Sci*, 3, 90-101.
- [9] Dogan, M. (2011). Delamination failure of steel single angle sections. *Engineering Failure Analysis*, 18(7), 1800-1807.
- [10] Bramfitt, B., & Marder, A. (1977). A study of the delamination behavior of a very low-carbon steel. *Metallurgical transactions A*, 8, 1263-1273.
- [11] Liu, Y., Shao, Z., & Mori, T. (2021). Development of nickel based cermet anode materials in solid oxide fuel cells—Now and future. *Materials Reports: Energy*, 1(1), 100003.
- [12] Kawasaki, A., & Watanabe, R. (1997). Concept and P/M fabrication of functionally gradient materials. *Ceramics international*, 23(1), 73-83.
- [13] Angelopoulos, V., Hirsch, M., & Weihmann, C. (2018). A parametric study on PM gear rolling densification simulations coupled with experimental results. Proceeding of the World Conference on Powder Metallurgy,
- [14] Klocke, F., & Löpenhaus, C. (2016). Densifying PM gears by shot peening. European Congress and Exhibition on Powder Metallurgy. European PM Conference Proceedings,
- [15] Gelbstein, Y., Dashevsky, Z., & Dariel, M. (2007). Powder metallurgical processing of functionally graded p-Pb1– xSnxTe materials for thermoelectric applications. *Physica B: Condensed Matter*, 391(2), 256-265.
- [16] Kratina, O., Stoček, R., Zádrapa, P., & Sathi, S. (2021). The Effect of Polyglycols on the Fatigue Crack Growth of Silica-Filled Natural Rubber. *Fatigue Crack Growth in Rubber Materials: Experiments and Modelling*, 39-55.
- [17] Bolton, W. (2013). *Engineering materials technology*. Elsevier.